Controlling Neutral Mixtures: Thin Film Deposition via Laser Ablation and Selective Ionization of $K_4In_4Sb_6$

Valentin Panayotov, Teresa L. T. Birdwhistell,† and Brent Koplitz*

Department of Chemistry, Tulane University, New Orleans, Louisiana 70118

Received October 7, 1997. Revised Manuscript Received January 15, 1998

We present experimental results on a technique that combines laser ablation with selective ionization in order to generate and subsequently separate neutral mixtures. For example, in the laser ablation (λ = 308 nm) of $K_4In_4Sb_6$, irradiation of the ablation plume with 248 nm laser light induces selective ionization of potassium. Subsequent electric field extraction leads to macroscopic depletion of potassium from the ablation plume. Quantification via scanning Auger electron spectroscopy of thin films deposited from such ablation plumes reveals that even without optimization of the spatial overlap between the ablation plume and the ionization laser, the technique leads to ~60% removal of potassium. While at present it is not clear whether conditions exist for full quantitative removal of the potassium, it is apparent that control over the neutral plume has been exerted.

I. Introduction

In a variety of chemical situations, controlling the composition of a mixture is a desirable outcome. When ions are involved, electric and/or magnetic fields can be utilized to exert influence over the system. With neutral mixtures, however, control is often much more elusive. Recently, we presented experimental results on a novel technique[1,2] (referred to as the ablation/ionization scheme) that utilizes laser ablation and subsequent selective ionization to control neutral systems, the example being I−III−V Zintl compounds.[3,4] Selective ionization of the group I element enables one to change the composition of a gas-phase plume in a controlled fashion. In the present work, macroscopic control over the ablation plune is demonstrated. Briefly, the principle of the method can be described as (i) laser ablation of a I−III−V Zintl compound, followed by (ii) removal of the group I element via selective gas-phase laser ionization and extraction in an electric field, and (iii) subsequent redeposition of the remaining group III and group V elements. In the present paper, we report on continuing efforts in our group to explore the feasibility of using laser-based methods to alter the composition of neutral mixtures.

The ablation/ionization scheme relies on selective ionization of only the group I element in a plume arising from laser ablation of a I−III−V Zintl compound. In principle, such selectivity can be achieved with laser radiation possessing a photon energy above the ionization potential of the group I element and below that of the group III and group V elements. For a variety of I−III−V Zintl compounds (e.g., $K_4In_4Sb_6$, $K_3Ga_3As_4$, and Rb·Ga·Sb), conditions have been found for reproducible ablation and selective laser ionization/removal of the group I element from its ablation plume.[1,5] However, these studies have been conducted in the ionization region of a time-of-flight mass spectrometer (TOFMS) and do not determine whether the selective removal effect can be scaled macroscopically, since laser ionization within the TOFMS utilizes only a small volume of a tight laser focus (necessary for high mass spectral resolution). In contrast, "macroscopic" removal of the group I element requires an experimental geometry in which a majority of the ablation plume is effectively irradiated by the ionization laser.

Within the materials community, there is considerable interest in a variety of dopants in many applications.[6−10] Likewise, III−V multilayered materials are commonplace. Eventually, if one can adjust the amount of potassium (or other element of choice) removed *on a shot-to-shot basis* and over a wide range, then a potentially powerful doping technique is available with applications ranging from the fabrication of doped gradients to layered materials. Selective ionization within an ablated plume offers this capability. Since I−III−V Zintl materials represent uniformly mixed precursors possessing an element with a low ionization potential, they constitute a good choice for addressing macroscopic control of a neutral mixture.

† Address: Department of Chemistry, Xavier University, New Orleans, Louisiana 70125.

(1) Panayotov, V.; Hamar, K.; Birdwhistell, T. L. T.; Red, C.; Dillon, J.; Dennison, D.; Barnes, A. P.; Koplitz, B. *Appl. Phys. Lett.* **1995**, *66*, 2241.

(2) Panayotov, V.; Hamar, K.; Birdwhistell, T. L. T.; Koplitz, B. *Proc. SPIE* **1995**, *2547*, 328.

(3) Schafer, H. *Annu. Rev. Mater. Sci.* **1985**, *15*, 1.

(4) (a) Birdwhistell, T. L. T.; Stevens, E. D.; O'Connor, C. J. *Inorg. Chem.* **1990**, *29*, 3892. (b) Birdwhistell, T. L. T.; Klein, C. L.; Jeffries, T.; Stevens, E. D.; O'Connor, C. J. *J. Mater. Chem.* **1991,** *1*, 555.

(5) Panayotov, V.; Hamar, K.; Red, C.; Birdwhistell, T. L. T.; Koplitz, B. *J. Appl. Phys.*, in press.

(6) Neufeld, E.; Sticht, A.; Brunner, K.; Abstreiter, G.; Holzbrecher, H.; Bay, H.; Buchal, Ch. *Appl. Phys. Lett.* **1997**, *71*, 3129.

(7) Talin, A. A.; Felter, T. E.; Devine, D. J. *J. Vac. Sci. Technol. B* **1992**, *13*, 448.

(8) Thaik, M.; Hömmerich, U.; Schwatz, R. N.; Wilson, R. G.; Zavada, J. M. *Appl. Phys. Lett.* **1997**, *71*, 2641.

(9) Sahana, M.; Hegde M. S.; Vasathacharya, N. Y.; Prasad, V.; Subramanyan, S. V. *Appl. Phys. Lett.* **1997**, *71*, 2701.

(10) Kim, T. J.; Holloway, P. H.; Kenik, E. A. *Appl. Phys. Lett.* **1997**, *71*, 3835.

S0897-4756(97)00668-6 CCC: $15.00
Published on Web 03/13/1998

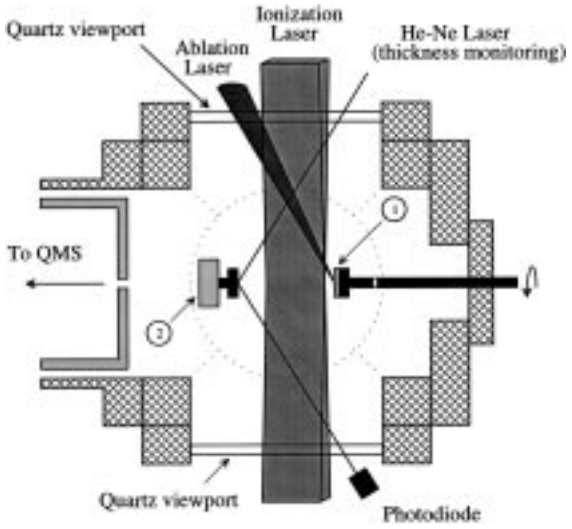

Figure 1. Top view schematic of the high-vacuum ablation/deposition system illustrating the geometry of laser irradiation. The ablation target is marked (1), and deposition occurs at the substrate (2). All laser beams lie in the plane of the figure.

However, it is not clear a priori whether macroscopic conditions can be found for selective removal of the group I species from a I−III−V Zintl material, since scaling of the ablation/ionization scheme does not necessarily constitute a trivial extrapolation of our previously reported ablation/ionization studies. In this paper, it is clearly demonstrated that macroscopic removal of the group I element (in this case potassium) after the laser ablation of $K_4In_4Sb_6$ is possible. Consequently, selective depletion of a neutral mixture via an ablation/ionization/deposition scheme is indeed a viable method by which neutral mixtures can be macroscopically controlled.

II. Experimental Section

The ablation/deposition studies were conducted in a diffusion-pumped high-vacuum system (base pressure $\sim 5 \times 10^{-8}$ Torr).[2] A schematic top view of the experimental setup is presented in Figure 1. The main chamber consists of a standard 6 in. "knife-edge" stainless steel cube. To provide a constantly fresh target surface during the ablation process, the ablation targets are mounted on a motorized rotary motion feedthrough (1 in Figure 1). The target stub can be insulated from ground with a Teflon coupler, thereby allowing it to be biased electrically. The deposition substrates (2 in Figure 1) are mounted on a linear motion feedthrough for manipulation under vacuum. The feedthrough accommodates six substrates as well as an oscillating quartz crystal sensor (Leybold, not shown) for thin-film thickness monitoring. Both the targets and the deposition substrates are mounted on standard VG ESCALAB stubs for compatibility with the sample-handling requirements pertaining to subsequent surface analysis. The ablation targets are prepared in inert atmosphere by pressing powdered $K_4In_4Sb_6$ to 0.5 in. diameter pellets, and the pellets are then attached with conductive carbon pads to the sample stubs. The deposition is carried out directly on the surface of polished (1200 grid, ~200 nm surface roughness as measured with a Tencor stylus profilometer) aluminum stubs that have been thoroughly cleaned and gold plated. Since the compound is air and moisture sensitive, it is introduced into the chamber through a quick-access loading port (not shown) covered with a glovebag and under a backstream of argon.

Laser beams are introduced into the chamber through custom-designed 4 in. quartz viewports. A XeCl excimer laser (λ = 308 nm, Lambda Physik) serves as the ablation source. It is moderately focused (f.l. = 25 cm) to ~2 mm^2 on the target surface. Typically, ~3 mJ of photon energy is transmitted to the target per pulse, producing laser power densities upon focusing of ~10 MW/cm^2. The output from a KrF excimer laser (λ = 248 nm, Questek), typically 10 mJ incident per pulse, is cylindrically focused with a barrel lens (f.l. = 25 cm) and is used for ionization. Due to the difficulties inherent in estimating the actual size of the laser focus, the resulting power densities upon focusing are obtained only as a rough estimate. A stand-alone electrode assembly (not shown) provides the electric field necessary for diverting the positive ions from the ablation plume. The assembly is primarily a metal plate with a central hole (1 cm) covered by a wire mesh that allows the ablation plume to pass. Biased at +1000 V with respect to the grounded chamber, the plate lies between the ablation target and the deposition substrate. With respect to Figure 1, the plate is perpendicular to the plane of the paper. In general, the electric field gradient is sufficient for removing neutral atoms that have been ionized by the ionization laser. However, the act of ablation can generate energized ions that exceed the repeller voltage (+1000 V) if care is not taken, so the ablation plume should be characterized and monitored with respect to both neutrals and ions.

Under typical experimental conditions, deposition rates of ~0.5 Å/s are achieved, yielding film thicknesses on the order of 100 nm in deposition times of ~30 min. To monitor in situ thin-film growth during deposition, the reflection from an energy-stabilized, linearly-polarized He−Ne laser (Melles Griot) is continuously measured with a photodiode (Thorlabs Inc.), amplified, and recorded on a chart recorder. For monitoring of the photoproducts responsible for thin-film deposition,[11,12] the system is equipped with a differentially pumped quadrupole mass spectrometer (Extrel C-50). It is important to note that the detection in this setup is not accomplished in situ during the deposition, but before and/or after the film is deposited by pulling up the substrate holder and exposing the ablation spot to the centerline extraction axis of the quadrupole mass spectrometer.

For surface analysis, the samples are transferred under inert atmosphere to the preparation chamber of a standard VG ESCALAB MARK II surface analysis instrument and then loaded in the analysis chamber, which is equipped with an LEG200 scanning electron source that has a minimum electron beam diameter of ~2000 Å. Auger electron spectroscopy (AES) data are collected with a primary beam energy of 5 keV and in a 1:4 constant retard ratio mode. The data are then transferred from the VG ESCALAB instrument to an IBM-PC with which custom-built software is used for subsequent data processing.

III. Results and Discussion

Given the relative ionization potentials (4.34, 5.79, and 8.64 eV for K, In, and Sb, respectively),[13] the ionization laser (KrF; 5.0 eV) is clearly above the ionization potential of atomic potassium and below that of atomic indium and antimony. As a result, selective removal of potassium is not only theoretically possible, but it has been dramatically demonstrated.[1] However, the presence of higher order neutral species (e.g., dimers and trimers) and two-photon ionization processes constitute possible complications in what may appear to be a straightforward procedure. Consequently, it is desirable to address the degree of control that one can exert over a neutral mixture by measuring to what

(11) Panayotov, V.; Kelly, M. C.; Gomlak, G. G.; Birdwhistell, T. L. T.; Koplitz, B. *Mater. Res. Soc. Symp. Proc.* **1997**, *441*, 469.
(12) Kelly, M. C.; Gomlak, G. G.; Panayotov, V.; Cresson, C.; Rodney, J.; Koplitz, B. *Appl. Surf. Sci.*, in press.
(13) Lide, D. R., Ed.*CRC Handbook of Chemistry and Physics*, CRC: Boston, 1990.

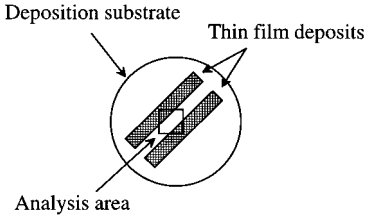

Figure 2. Schematic illustrating sample geometry for the subsequent deposition and surface analysis.

extent the deposited material is actually depleted in the targeted species, in this case potassium.

The deposition geometry for these experiments is depicted in Figure 2. A mask in the form of a narrow slit is used for deposition onto only a small area of the substrate, thereby resulting in a narrow stripe. Here, no attempt is made to remove the potassium. Next, the substrate is moved and another stripe is deposited under different deposition conditions, i.e., the potassium is actively removed. Deposition onto the same substrate during the same vacuum cycle ensures that the deposits receive identical pre- and post-treatment and gives a basis for comparison of their properties as a function of the deposition conditions only. Another advantage is that the deposits are not in contact with each other, thus making the migration of elements between them unlikely. For analysis, small-area AES is applied to study the composition of the individual deposits (stripes), and compositional maps are also produced from an area encompassing both of the deposits, as depicted in Figure 2.

Figure 3 presents the results from a scanning Auger microscopy study for two adjacent thin films deposited by laser ablation/ionization of $K_4In_4Sb_6$ according to the geometry shown in Figure 2. For this technique (known also as Auger imaging or element mapping),[14] the kinetic energies of the Auger transitions for the elements of interest are first determined using an Auger spectrum collected from the entire area. For each element to be analyzed, the spectrometer is fixed to an electron kinetic energy corresponding to that element's most significant Auger transition, and the interrogating electron beam is then scanned across the area of interest. Intensities for peak, *P*, and background, *B*, are collected, averaged as necessary, and stored for each pixel. The peak data alone are not sufficient, since the Auger peaks appear on a high background of backscattered electrons *and* of peaks at higher kinetic energies. The data on Figure 3 represent peak minus background intensities, $P - B$, after spike removal. (Note that spike removal is based on assigning a value to the spike from adjacent averaging of a user-defined neighboring region.) The negative intensity values result from measurements of the peak and background at adjacent energies and correspond to negligible surface concentration of the corresponding element. The spot size for this case is estimated at ~10 μm, and data points were acquired for a 128 × 128 matrix evenly spaced between the available 1024 × 1024 pixels.

The three plots in the left column of Figure 3 represent compositional surface maps of potassium, indium, and antimony, respectively. For this experiment, the film to the left within each subfigure has been deposited without ionization of the ablation plume. During the deposition of the film on the right within each subfigure, 248 nm laser ionization has been applied following a 10 μs delay with respect to the ablation pulse. It is apparent that the potassium intensity (top plot) for the film deposited *with* ionization is significantly reduced. Clearly, the potassium has been markedly depleted. In contrast, the indium and antimony intensities (middle and bottom plots) for the film deposited with ionization (to the right in each subfigure) have increased. This result is consistent with the fact that the *relative* concentrations of these elements on the surface should be higher in the absence of potassium and again indirectly confirms the removal of potassium. The presence of such high intensities from indium and antimony suggests that their deposition has not been significantly affected by the process of potassium removal. The combination of the three plots presents unambiguous evidence that *selective* removal of the group I element from a thin-film deposit has been achieved, while the group III and V elements have been redeposited with relatively little alteration.

A different depiction of these results can be achieved by plotting them in the form of surface images as presented with the three plots in the right column of Figure 3. These images correspond to the compositional surface maps of the left column and represent a top view projection of the data after two-dimensional interpolation and rescaling to 256 gray levels. One should bear in mind that although this type of projection resembles a scanning electron microscopy image, it is essentially a concentrational map for the corresponding element resulting from chemical analysis for each pixel, rather than a topological picture of the surface. The potassium image (top plot) reveals the film deposited with ionization (bottom right corner in this projection) as a less dense area which corresponds to reduced potassium concentration.

As seen, these images give more information on details not otherwise seen on the compositional maps. First of all, the surface-defect picture is clearly revealed. (The particular substrate used in this experiment—a gold-plated aluminum stub—developed surface defects, probably due to the poor adhesion of the gold underlayer.) An interesting effect is that the indium and antimony images reveal almost one and the same defect picture, different from the one for potassium. A detailed study of the composition and structure of this type of deposit is currently underway.

To quantify the degree of potassium removal, an AES spectrum was taken separately for each of the twin films. Procedurally, the interrogating electron beam size was enlarged to fill the central portion of the stripe being examined. The results for the potassium region taken at 10 μs ionization delay are presented in Figure 4, together with another study made with laser ionization delays of 5 and 7.5 μs. The trace for the film without ionization (ablation only) clearly exhibits the highest potassium concentration, while the traces with successive increase of the delay show reduction in the potassium concentration. Note that in each case, an "ablation only" area was measured and its intensity

(14) Briggs, D.; Seah, M. P., Eds. *Practical Surface Analysis By Auger and X-ray Photoelectron Spectroscopy*; Wiley: New York, 1983.

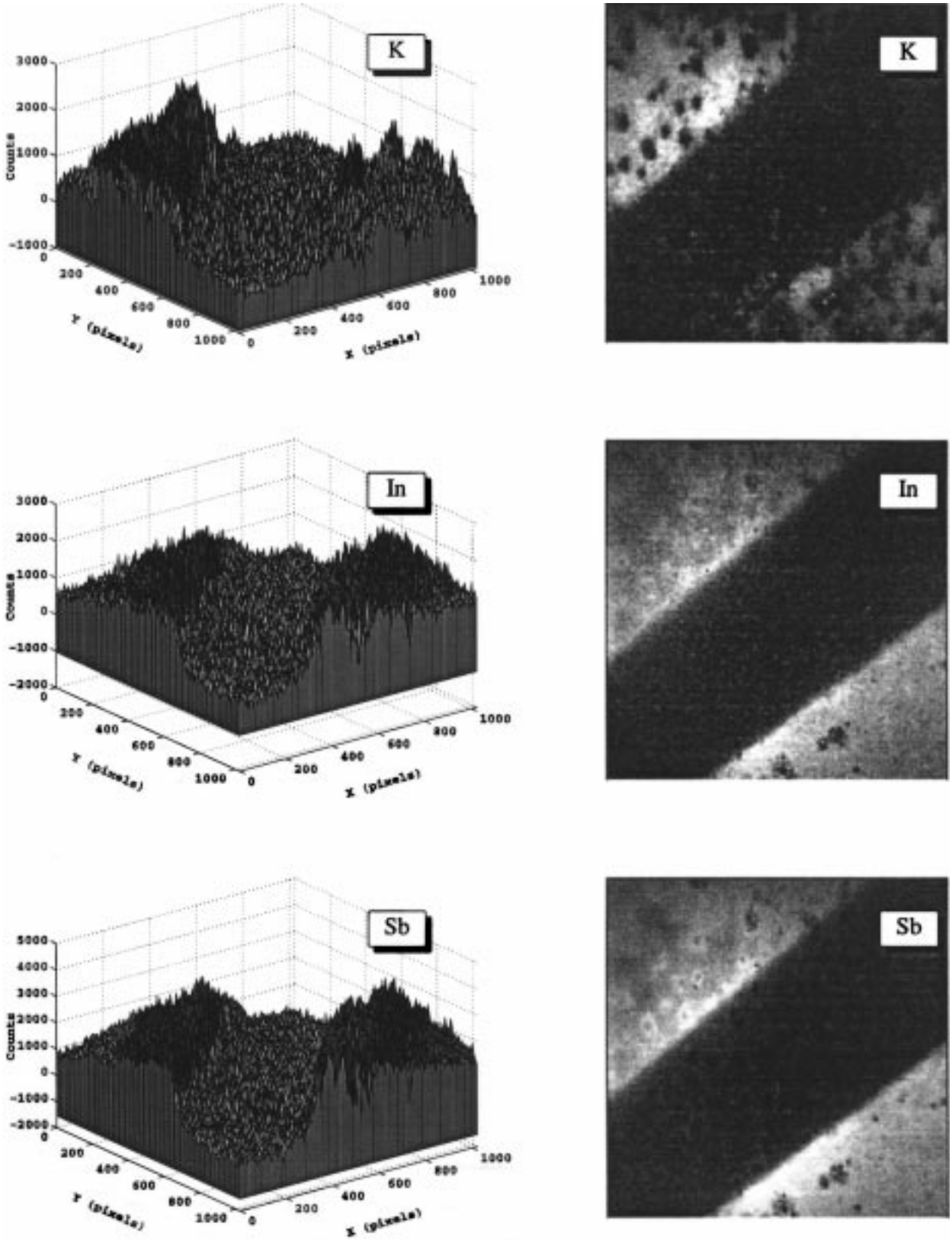

Figure 3. Auger compositional (left) and corresponding surface image (right, see text) maps of potassium, indium, and antimony for two adjacent thin films resulting from laser ablation of $K_4In_4Sb_6$ (see geometry in Figure 2). The film to the left in each subplot has been deposited *without* ionization of the ablation plume. Note that the intensity scales are different, corresponding to the surface concentrations and sensitivity factors for the different elements.

recorded as a calibrant, but only one is shown in order to maintain figure clarity. As seen, the effect of potassium removal is unambiguously expressed for the films produced with ionization. Absolute quantification of these data is hindered by the accuracy of Auger analysis—limited to not better than ±10% while relative concentration differences can be measured well within ±3% accuracy.[15] Here, the relative potassium intensities for the four films above, as derived from peak areas, are 100:77:63:42.

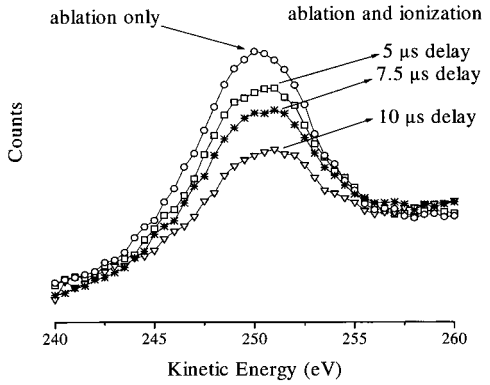

Figure 4. Auger spectra for thin films deposited by laser ablation of $K_4In_4Sb_6$. The topmost trace is for a film deposited without ionization (laser ablation only). The bottom three traces are for films deposited with different delays of the ionization laser. Note that just one ablation-only trace is shown for clarity.

We attribute the remaining potassium content in the films deposited with laser ionization to nonoptimization of our experimental conditions. Most likely, transmission of potassium from the target to the deposits has been caused by several factors. (1) There may be insufficient ionization laser power density throughout the focal volume, leaving potassium atoms in the gas phase unexposed and un-ionized. (2) An unoptimized match can exist between the position and size of the irradiation volume of the ionization laser with respect to the ablation plume. The spatial extent of the ablation plume may be too long in comparison to the focal spread of the ionizing laser beam. (3) The ablation source in the ultraviolet region (308 nm) can cause highly energetic ablation plumes and plasma generation. In this case, positive ions with kinetic energies greater than the repeller voltage (+1000 V) may be created. Consequently, all positive ions would not be efficiently diverted away from the deposits.

In principle, these problems are tractable. With systematic characterization and further experimentation, it is expected that an improvement in the degree of potassium removal can be achieved in a straightforward manner. The above considerations are relevant not only to the described depositions from $K_4In_4Sb_6$ but also to the proposed ablation/ionization scheme in general. At present, however, it is not clear whether conditions exist for full, quantitative removal of the group I element from the resulting thin films. On the other hand, it is apparent that control over a neutral mixture has been exerted macroscopically, and the prospects for the method as a vehicle for controlling other systems are encouraging.

IV. Conclusions

The demonstrated significant removal of potassium from thin films deposited by laser ablation/ionization of $K_4In_4Sb_6$ represents clear experimental evidence for macroscopic selective depletion of a group I element from a Zintl phase ablation plume. The degree of removal achieved here is estimated to be ~60% of the total amount of potassium, as determined from a film deposited without ionization. The present study is of preliminary character, and no special optimization for potassium removal from the solid phase has been performed yet. However, the degree of removal can be considered as evidence of the viability of the proposed ablation/ionization technique for the macroscopic control of neutral mixtures.

Acknowledgment. This project was supported by the Department of Energy, the National Science Foundation through the Center for Photoinduced Processes, Tulane's Center for Bioenvironmental Research (supported by the Department of Defense), the LaSPACE program, and the Louisiana Board of Regents via its LEQSF program.

CM970668L

(15) Bishop, H. E. Auger Electron Spectroscopy. In *Methods of Surface Analysis*; Walls, J. M., Ed.; Cambridge University Press: Cambridge, 1989; p 87.